Springer

Journal of Mechanical Science and Technology

Journal of Mechanical Science and Technology 23 (2009) 2320~2329

www.springerlink.com/content/1738-494x
DOI 10.1007/s12206-009-0523-0

Influences of equal biaxial tensile loads on the stress fields near the mixed mode crack †

Dong-Chul Shin[1], Jeong-Hwan Nam[2], Jai-Sug Hawong[2,*] and Joon-Hyun Lee[1]

[1]*School of Mechanical Engineering, Pusan National University, 30, Jangjeon, Geumjeong, Busan 609-735, Korea*
[2]*School of Mechanical Engineering, Yeungnam University, 214-1, Dae, Gyoungsan, Gyoungbuk, 712-749,*

(Manuscript Received January 15, 2009; Revised April 8, 2009; Accepted April 28, 2009)

Abstract

A hybrid method for photoelasticity is introduced and applied to the plane problems of isotropic polycarbonate plates with a central crack under uniaxial and equal biaxial tensile loads. Also, the influences of equal biaxial tensile loads on the isochromatic fringes, stress fields and stress intensity factors near the mixed mode crack-tip have been investigated. The results show that, when an equal lateral tensile load is added to the specimen under uniaxial tensile load, the asymmetric isochromatic fringes about the line of crack gradually become symmetric, and the slope of the isochromatic fringe loop near the crack-tip is inclined towards the crack surface according to the increasing of the inclined angle of crack. Furthermore, the shapes of distribution of all stress components are changed from asymmetric to symmetric. In the equal biaxial tensile load condition against the uniaxial tensile load condition, the values of stress intensity factors are changed little, and only the region of compressive stress of σ_x / σ_0 is changed when $\beta = 0^o$, but the values of K_I / K_0 are increased and those of K_{II} / K_0 become almost zero, namely, we have the mode I condition when $\beta = 15^o \sim 45^o$.

Keywords: Stress fields; Stress intensity factors; Mixed mode crack; Equal biaxial tensile load; Hybrid method for photoelasticity

1. Introduction

To date, there have been various theoretical methods and experimental methods to analyze the stresses in elasticity plane problems, and although these can give the correct solutions for relatively simple problems, they cannot, however, give the correct solutions for irregular geometric shapes and complex loads found in realistic, practical problems. The solution is to use a hybrid method that combines the merits of the experimental, numerical and analytical methods, etc., and many studies have been carried out as presented next.

Pian, Tong and Luk [1] analyzed the elastic crack problem using hybrid elements in the finite element method. Chandrashekhara and Jacob [2] suggested the experimental-numerical hybrid method for the stress analysis of the plane problem of orthotropic material. Smith, Post, Hiatt and Nicoletto [3] measured the deformation in the vicinity of a crack tip using the hybrid approach with the moire method. Shin et al. [4-6] studied the stress fields and stress intensity factors (SIFs) near the crack-tip in elastic materials and orthotropic materials using the hybrid method for transmission type photoelasticity. But, there has been little research on biaxial loading problems using the hybrid concept, especially, hybrid method for photoelasticity.

In the actual structural components or machine parts, the loading conditions are rarely uniaxial, but typically biaxial or even triaxial. Therefore, experimental studies on the various biaxial stress states, which are more actual stress state rather than uniaxial stress, must be carried out. In the study of biaxial

† This paper was recommended for publication in revised form by Associate Editor Chongdu Cho
* Corresponding author. Tel.: +82 53 810 2445, Fax.: +82 53 810 4627
E-mail address: jshawong@ynu.ac.kr

loads, Kim and Crasto [7] studied the interaction between both longitudinal tension and transverse compression, and longitudinal compression and transverse compression, using the graphite-epoxy mini-sandwich specimens.

Swanson and Christoforou [8, 9] have also conducted similar research using tubular specimens, and found that there is little interaction between longitudinal loading and transverse loading when matrix-dominated modes are restrained. Lim and Choi et al. [10] studied the theory of the biaxial load effects on crack extension in anisotropic solids, using the maximum circumferential tensile stress criterion. Shimamoto et al. [11] obtained the stress intensity factors according to various biaxial load ratios in the cruciform specimens of elastic and anisotropic material by the photoelastic and caustic methods. Shin et al. [12] suggested the improved cruciform biaxial specimen with slots in the loading parts and ascertained its validity by means of finite element analyses and photoelastic experiments. Shin's paper [12] showed that, even though the load biaxiality ratio γ =1, the stress biaxiality ratios in central region of cruciform biaxial specimen differ according to the position from the center of specimen. Therefore, we use the word, "equal biaxial tensile load" that is, not "equal biaxial tensile stress."

However, there has been little research on the influences of equal biaxial tensile loads on the isochromatic fringes, near crack tip stress fields and stress intensity factors in the mixed mode using the photoelastic experiment, not to mention the hybrid method for photoelasticity. Thus, this paper presents a proposed study of these phenomena using the hybrid method for photoelasticity.

2. Basic theory

2.1 Near crack-tip stresses for linear elastic isotropic material

Stress components of the plane problem, obtained from the Airy stress function for linear elastic isotropic material, are [13]

$$\begin{aligned}\sigma_x &= \mathrm{Re}\left[2\phi'(z) - \bar{z}\phi''(z) - \varphi'(z)\right]\\ \sigma_y &= \mathrm{Re}\left[2\phi'(z) + \bar{z}\phi''(z) + \varphi'(z)\right]\\ \tau_x &= \mathrm{Im}\left[\bar{z}\phi''(z) + \varphi'(z)\right]\end{aligned} \tag{1}$$

where $\phi(z)$ and $\varphi(z)$ are arbitrary harmonic analytic functions with $z = x + iy$.

Since the stress functions $\phi(z)$ and $\varphi(z)$ are analytic functions, they can be expressed by the power series as follows:

$$\phi(z) = \sum_{n=0}^{N} C_n z^{\frac{n}{2}}\ , \quad \varphi(z) = \sum_{n=0}^{N} D_n z^{\frac{n}{2}} \tag{2}$$

From the traction-free condition on the crack surface ($\sigma_\theta = \tau_{r\theta} = 0$), we have

$$\begin{aligned}\sigma_\theta + i\tau_{r\theta} &= \phi'(z) + \overline{\phi'(z)} + e^{2i\theta}\left[\bar{z}\phi''(z) + \varphi'(z)\right]\\ &= \sum_{n=1}^{N}\frac{n}{2}\left\{C_n z^{\frac{n}{2}-1} + \overline{C_n}\,\bar{z}^{\frac{n}{2}-1}\right.\\ &\quad\left. + e^{2i\theta}\left[\bar{z}\left(\frac{n}{2}-1\right)C_n z^{\frac{n}{2}-2} + D_n z^{\frac{n}{2}-1}\right]\right\} = 0\end{aligned} \tag{3}$$

Thus substituting $\pm\pi$ for θ into Eq. (3), we obtain

$$D_n = -\left\{\frac{n}{2}C_n + (-1)^n\overline{C_n}\right\} \tag{4}$$

As shown in Eq. (4), if C_n is determined, $\phi(z)$ and $\varphi(z)$ can be determined through Eqs. (2) and (5). Then we can define the stress components expressed by the power series as follows:

$$\begin{aligned}\sigma_x &= \sum_{n=1}^{N}\mathrm{Re}\left\{C_n\left[2f(n,z) - g(n,z)\right] + (-1)^n\overline{C_n}f(n,z)\right\}\\ \sigma_y &= \sum_{n=1}^{N}\mathrm{Re}\left\{C_n\left[2f(n,z) + g(n,z)\right] - (-1)^n\overline{C_n}f(n,z)\right\}\\ \tau_{xy} &= \sum_{n=1}^{N}\mathrm{Im}\left\{C_n g(n,z) - (-1)^n\overline{C_n}f(n,z)\right\}\end{aligned} \tag{5}$$

where

$$f(n,z) = \frac{n}{2}z^{\frac{n}{2}-1},\quad g(n,z) = \frac{n}{2}\left\{\bar{z}\left(\frac{n}{2}-1\right) - \frac{n}{2}z\right\}z^{\frac{n}{2}-2}$$

2.2 Hybrid method for photoelasticity

To apply Eq. (5) to the photoelastic experiment, substituting it into the stress optic law [14] gives

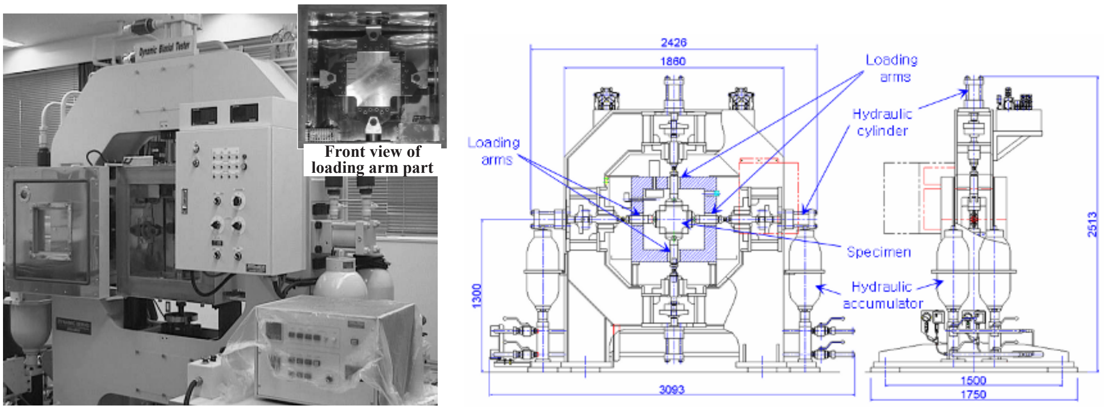

Fig. 1. Photograph and schematic drawings of the biaxial loading device.

$$\begin{aligned}\left(\frac{f\cdot N_f}{t}\right)^2 &= \left(\sigma_x-\sigma_y\right)^2+\left(2\tau_{xy}\right)^2\\ &=\left\{2\sum_{n=1}^{N}a_n\,\mathrm{Re}\left[f_c(n,z)-g_c(n,z)\right]\right.\\ &\quad\left.+2\sum_{n=1}^{N}b_n\,\mathrm{Im}\left[f_c(n,z)+g_c(n,z)\right]\right\}^2\\ &\quad+\left\{2\sum_{n=1}^{N}a_n\,\mathrm{Im}\left[g_c(n,z)-f_c(n,z)\right]\right.\\ &\quad\left.+2\sum_{n=1}^{N}b_n\,\mathrm{Re}\left[f_c(n,z)+g_c(n,z)\right]\right\}^2\end{aligned} \tag{6}$$

where

$$f_c(n,z)=(-1)^n f(n,z),\quad g_c(n,z)=g(n,z)$$

where f is the stress fringe value of the photoelastic specimen, t is the thickness of specimen, z is the position from the crack-tip, and N_f is the isochromatic fringe order at the position z. Therefore, the unknown quantities in Eq. (6) are only the complex coefficients $C_n=a_n+ib_n$. The real numbers a_n and b_n can be obtained by the nonlinear least squares method for the photoelastic experiment [5]. Thus, substituting the obtained C_n into Eq. (4), we can calculate the D_n and determine the stress functions $\phi(z)$ and $\varphi(z)$ from Eq. (2). Then, applying the C_n to Eq. (5) gives the stress components near the crack-tip. This process is known as the hybrid method for photoelasticity for linear elastic isotropic material.

The relationships between the SIFs and the complex coefficients C_n are given in Eq. (7) [4, 6]

$$\begin{aligned}&K_0=\sigma_0\sqrt{\pi a},\\ &K_I=\sqrt{2\pi}a_1,\quad K_{II}=\sqrt{2\pi}b_1\end{aligned} \tag{7}$$

where σ_0 is tensile stress applied to the specimen, a is half of the crack length and $C_1\left(=a_1+ib_1\right)$ is the complex coefficient when n=1.

3. Experiment and experimental method

For this research, a hydraulic type biaxial loading device was used, which was developed by the authors (see Fig. 1) [15]. The device can produce both dynamic and static state, and control various load ratios between X-Y axes under biaxial loading condition since the two axes are independent of each other.

The photographs of isochromatic fringe pattern were taken by CCD camera system (FASTCAM-Net 500C/1000C/ Max: PHOTRON).

The photoelastic specimens were poly-carbonate plate (PS1S, Measurements Group, Inc) and had been manufactured by end-milling by using a vertical machining centre (MC) as shown in Fig. 2. For all the specimens, the height and width are 300 mm, the thickness (t) is 3 mm and the width of specimen arms (w) is 140 mm.

Almost a whole central crack was machined, with an inclined angle, β =0°, 15°, 30°, 45° by a long end-mill of 0.8 mm diameter, and then the crack was polished with a razor until the total length of crack ($2a$) was 30 mm, in order to make it similar to a natural crack. The stress fringe value (f) of specimen used in this research is 6.993 kN/m-fringe. It is important to note that even though the equal biaxial load is applied to the specimen, the state of stress in the central test region of the specimen is no equal biaxial stress condition.

Photoelastic experiments under biaxial tensile loading ($P_{X'}:P_{Y'}$ =1) were carried out after those under

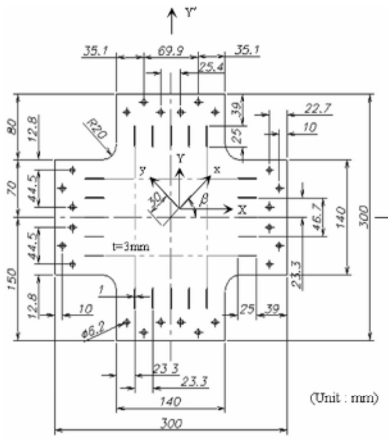

Fig. 2. Dimension of cruciform specimen.

uniaxial tensile loading ($P_{X'} : P_{Y'}$ =0) were accomplished.

Note that the (X', Y') is a Cartesian coordinate system in which the X'-axis is parallel to the direction of the horizontal arms of the biaxial loading device and the central point of specimen is the origin, but the (X, Y) is one in which X-axis is parallel to the horizontal line and the crack tip is the origin. In addition, the (x, y) is a coordinate system where the x-axis coincides with the line of crack and the origin is the crack tip, as shown in Fig. 2.

Doyle et al. [16] had pointed out that the region for photoelastic isochromatic fringe data collection is very important to solve the unknown variables in fracture problems. Therefore, in order to achieve precise experimental results in this research, we should uniformly select most of the 300 experimental data on the x.0 or x.5 fringe orders of the isochromatics in the region, where the distance from the crack tip is greater than 0.2~0.3 mm, and r/a is less than 0.7, and we should expand the power series of stress function to n=11~13.

4. Experimental results and discussion

Fig. 3 shows that the actual isochromatic fringe patterns obtained from photoelastic experiments, and the regenerated ones calculated from the obtained stress components through the hybrid method for photoelasticity, when the uniaxial tensile load (γ =0), and the biaxial tensile load (γ =1) were applied to the biaxial specimens with a central crack of inclined angle, β =0^o ~ 45^o . Here, the γ means the biaxial load ratios ($P_{X'}/P_{Y'}$). The whole actual isochromatics on the left sides of each case were represented, and the areas marked by "□" are the regions selected for comparing regenerated isochromatics with actual ones. The photos on the right side of each case are the actual isochromatics (upper part) and regenerated one (lower part), respectively, and "+" marks in the generated one indicate the positions where the isochromatic fringes were measured on each half fringe order. As shown in Fig. 3, the regenerated isochromatic fringes are almost identical to the actual ones, and "+" marks are located at the center of x.0 (black) or x.5 (white) order isochromatics. Thus, it can be verified that the hybrid method for photoelasticity used in this research is effective.

It can be seen from the isochromatic fringe patterns (see Fig. 3(a), (c), (e), (g)) in the selected regions in cases of uniaxial tensile loading (γ =0), as the inclined angle of crack, β increases, the size of the same order loop of isochromatics above and below the positive X-axis (i.e., the horizontal line in front of crack tip) becomes smaller, and the slope of isochromatics' loop is slanted toward the opposite side to the crack surface (i.e., x-axis). Also, it should be noted that the loop of isochromatics ahead of the crack tip is nearly symmetric about the X-axis.

For the cases of biaxial tensile loading (γ =1) (Fig. 3(b), (d), (f), (h)), on the other hand, the size of the same order loop of isochromatics above and below the positive x-axis (i.e., the line of crack) at each angle, is almost identical, and the slope of isochromatics' loop is slanted toward the crack surface. It should be noted that, contrary to the cases of γ =0, the loop of isochromatics near the crack tip is almost symmetric about the x-axis, namely, under the mode I condition, unlike uniaxial tensile loading. It can also be seen that the phenomenon that the two isochromatic fringes of N=0 (black spots in circular isochromatics) above and below the crack surface, become one when the inclined angle of crack, β is more than 30^o.

In addition, when an equal lateral tensile load is added to the specimen under uniaxial tensile loading, the isochromatic fringe loops, which were asymmetrical about the x-axis (but symmetrical about the X-axis in front of crack), gradually become symmetric, and the slope of isochromatic fringe loop near the crack-tip is inclined toward the crack surface, according to the increase of inclined angle of crack. Namely, the mixed mode condition is changed into the mode I condition.

Figs. 4 and 5 show contours of the normalized

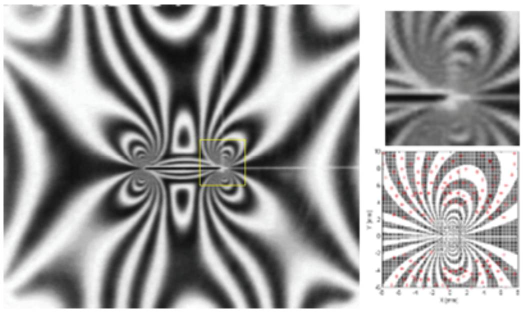

(a) $P_{X'} : P_{Y'}$ =0 kg : 400 kg ($\beta = 0^o$)

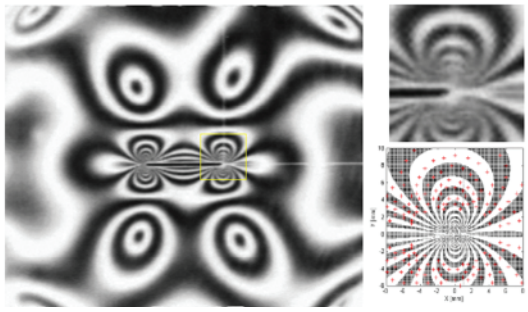

(b) $P_{X'} : P_{Y'}$ =400 kg : 400 kg ($\beta = 0^o$)

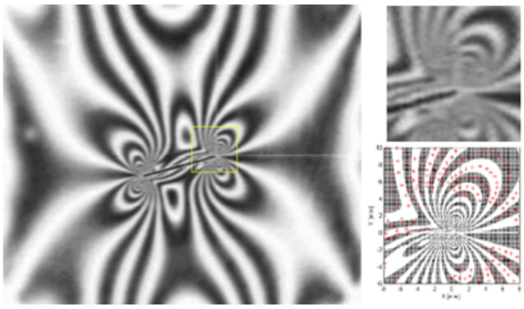

(c) $P_{X'} : P_{Y'}$ =0 kg : 400 kg ($\beta = 15^o$)

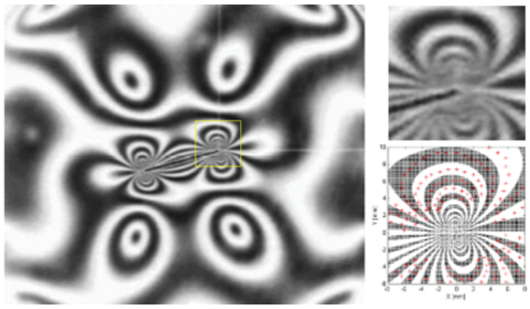

(d) $P_{X'} : P_{Y'}$ =400 kg : 400 kg ($\beta = 15^o$)

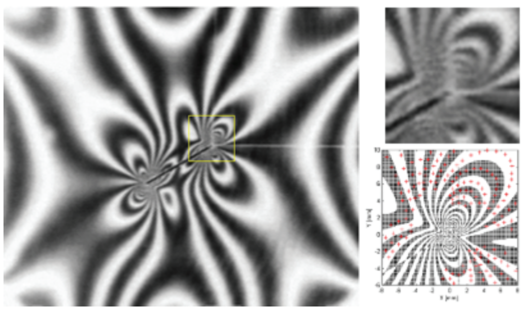

(e) $P_{X'} : P_{Y'}$ =0 kg : 400 kg ($\beta = 30^o$)

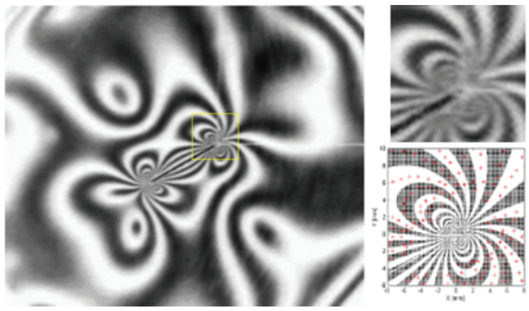

(f) $P_{X'} : P_{Y'}$ =400 kg : 400 kg ($\beta = 30^o$)

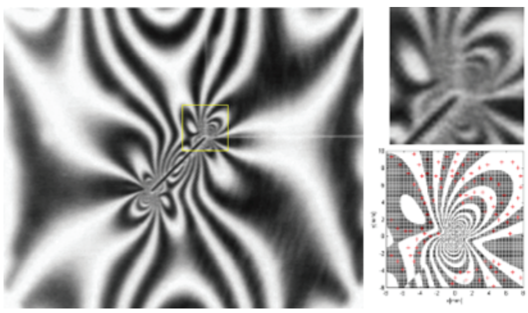

(g) $P_{X'} : P_{Y'}$ =0 kg : 400 kg ($\beta = 45^o$)

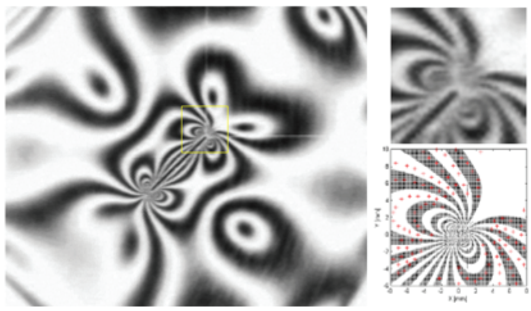

(h) $P_{X'} : P_{Y'}$ =400 kg : 400 kg ($\beta = 45^o$)

Fig. 3. Actual isochromatics and regenerated isochromatics for isotropic material.

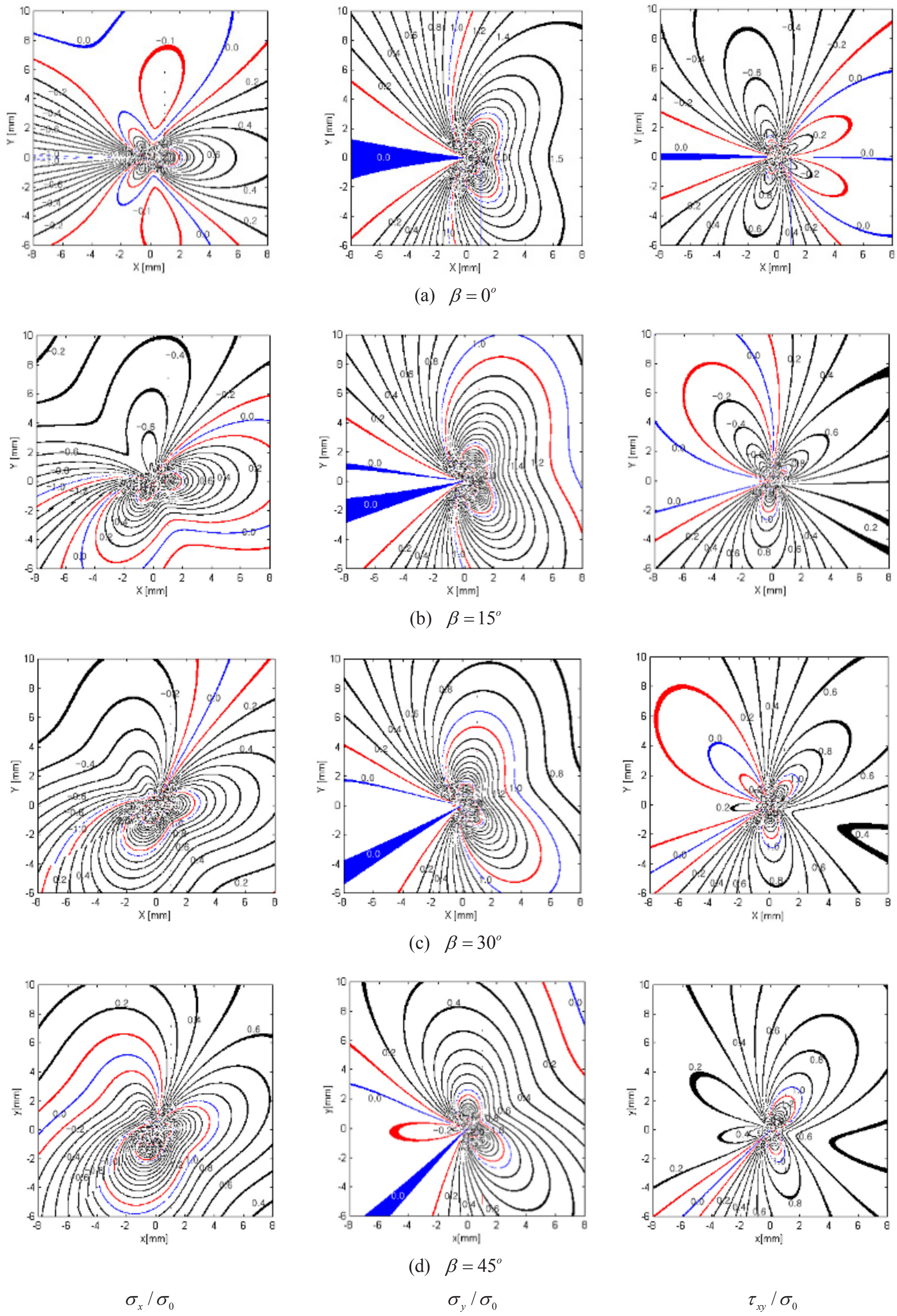

Fig. 4. Contour lines of normalized near crack tip stresses with biaxial load ratios, γ =0 ($P_{X'}$: $P_{Y'}$ = 0 kg : 400 kg) obtained from the hybrid method for photoelasticity.

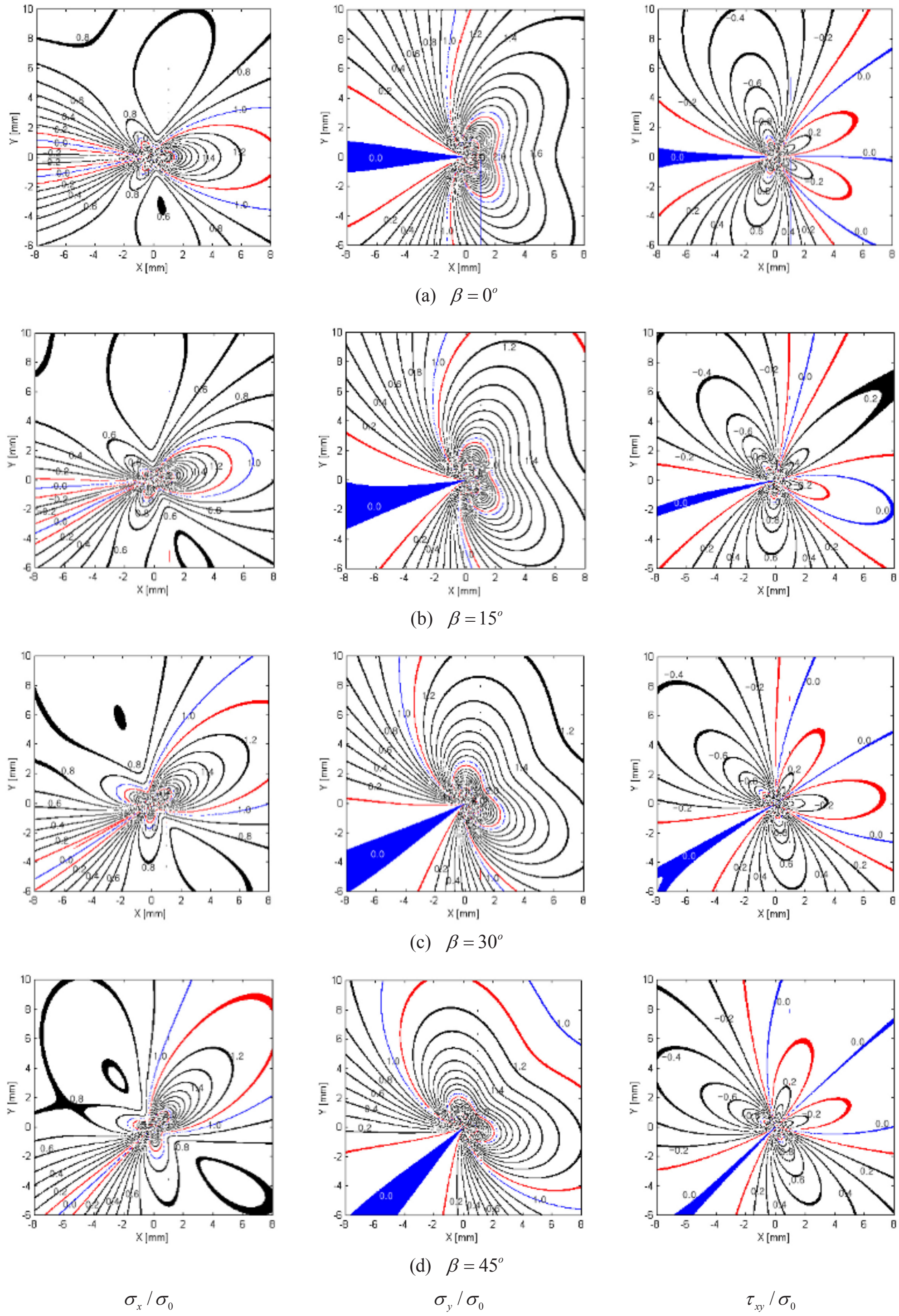

(a) $\beta = 0^o$

(b) $\beta = 15^o$

(c) $\beta = 30^o$

(d) $\beta = 45^o$

σ_x / σ_0 σ_y / σ_0 τ_{xy} / σ_0

Fig. 5. Contour lines of normalized near crack tip stresses with biaxial load ratios, γ =1 ($P_{X'} : P_{Y'}$ = 400 kg : 400 kg) obtained from the hybrid method for photoelasticity.

stress components (σ_x/σ_0 , σ_y/σ_0 and τ_{xy}/σ_0) in the vicinity of the crack tip, obtained from the hybrid method for photoelasticity in the cases of γ =0 and γ =1 in the Fig. 3, respectively. The stresses are normalized by the applied far field stress ($\sigma_0 = P_Y/(w \cdot t)$), and the contour lines have been increased by 0.1 steps. Remembering that the (X, Y), in Figs. 4 and 5, is a Cartesian coordinate system, the X-axis is parallel to the horizontal line and the crack tip is the origin, as is mentioned above, and the stresses are calculated with respect to the Cartesian coordinate system (x, y), thus the crack surface (namely the negative x-axis) in each case has been rotated in β degrees counterclockwise to the negative X-axis. In Figs. 4 and 5, we can see that the values of σ_y and τ_{xy} on the crack surface are zero, that is, the traction-free condition is satisfied.

In Fig. 4 (γ =0), comparing the shapes and orders of contour lines of stress components according to the increase of the inclined angle of crack, it can be observed that, for the σ_x/σ_0 , the perfect symmetric stress contour about the line of crack (x-axis) when β =0° changes to asymmetric, and the necked part of "ω -shape" gradually becomes flat, and the region of the compressive stress above the crack surface gradually narrows. For the σ_y/σ_0 , the stress contour is changed into the shape rotated a little clockwise to the line of crack, and the region of the compressive stress above the crack surface appears, and gradually becomes wider, contrary to the σ_x/σ_0 . Next, in relation to the τ_{xy}/σ_0 , the stress contour is changed to asymmetric, and the slope of stress contours is gradually slanted counterclockwise to the X-axis, similarly to the σ_x/σ_0 , and the region of the compressive stress above the crack surface gradually narrows and disappears at β =45°.

In the case of Fig. 5 with γ =1, in contrast to Fig. 4, it can be seen that the distributions of all the stresses are symmetric about the line of crack (i.e., in the Mode I condition), and the shapes of the distribution are very similar to each other, regardless of the inclined angle of crack. Taking the x-axis (the line of crack) as a base line, the orders as well as the distribution shapes of stress contour lines for the σ_x/σ_0 and τ_{xy}/σ_0 are similar to each other. For the σ_y/σ_0 , the distribution shapes of stress contours are symmetric about the line of crack, but the value of the highest order at crack tip becomes smaller as the inclined angle of crack increases.

Comparing both cases of the uniaxial tensile loading and the equal biaxial tensile loading, in β =0°, the distribution shapes and the orders of stress contour lines are almost identical, except for the change of the compressive region of σ_x/σ_0 . In other words, when an equal lateral tensile load is added to the specimen under uniaxial tensile load with β =0°, only the change of the compressive region of σ_x/σ_0 occurs, thus consequently, the change of isochromatic fringe patterns is resulted from only the change of σ_x . For the cases of β =15° ~ 45°, the asymmetrical stress contours about the x-axis under uniaxial tensile loading are changed into symmetrical ones, and this transition might cause the change of the orders of the stress contours.

It is important to note that the mixed mode condition under the uniaxial tensile loading is changed into the mode I condition when the x-axis is taken as a base line, and that only the compressive region of σ_x/σ_0 is changed as compared with the contours of the stresses under uniaxial tensile loading with β =0°.

Fig. 6 represents the normalized stress intensity factors for each case of Fig. 3, which are calculated from the complex coefficients obtained from the hybrid method for photoelasticity and normalized by $K_0 (= \sigma_0 \sqrt{\pi a})$. Comparing the results of biaxial tensile load with those of uniaxial tensile loading, the value changes of K_I/K_0 and K_{II}/K_0 in case of β =0° are very small in this research condition as shown in Fig. 6. However, it is remarkable that the values of the mixed mode condition in γ =0, when β =15° ~ 45°, are changed into those of the mode I condition, that is, the values of K_{II}/K_0 become almost zero and the values of K_I/K_0 are increased. In addition, the values of K_I/K_0 in the equal biaxial

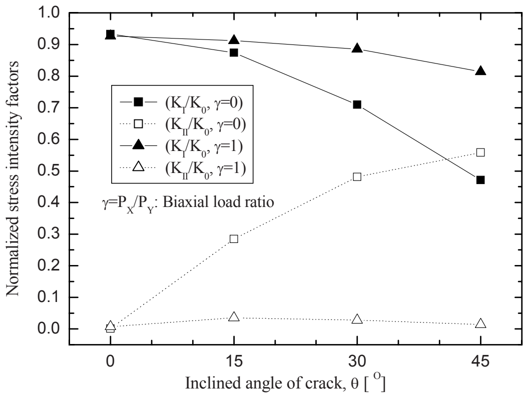

Fig. 6. Normalized stress intensity factors with the inclined angle of crack.

tensile loading become gradually smaller as the inclined angle of crack increases. The variation of SIFs in Fig. 6 is coincidental with one of the isochromatics in Fig. 3, and one of the stress contours in Figs 4 and 5.

5. Conclusions

The following conclusions were obtained through the study on the influences of the equal biaxial load on the stress components, and stress intensity factors in the vicinity of crack tip, when the uniaxial tensile load and the equal biaxial tensile load are subjected to the isotropic polycarbonate plates with the various inclined angle of crack.

1. The hybrid method for photoelasticity has been introduced and its validity for the biaxial tensile loading test was verified in this research.
2. As the equal lateral load is subjected to the specimen under uniaxial tensile loading, regardless of the inclined angle of crack, the isochromatic fringe loops which were asymmetric about the line of crack (but symmetric about the X-axis in front of the crack) become symmetric ones, i.e., mode I condition, and the slopes of isochromatic fringe loops near the crack-tip are inclined toward the crack surface, according to the increase of inclined angle of crack.
3. When $\beta = 0^o$, applying the equal lateral tensile load resulted only in the change of compressive region of σ_x / σ_0, but it did not affect the orders and the distribution shapes of stress contours of σ_y and τ_{xy}. Thus, the change of isochromatic fringe patterns was caused by the value change of σ_x.
4. When $\beta = 15^o \sim 45^o$, the asymmetrical stress contours about the line of crack (i.e. x-axis) under uniaxial tensile loading are changed into symmetrical ones, and only the compressive region of σ_x / σ_0 is changed as compared with the contours of the stresses under uniaxial tensile loading with $\beta = 0^o$.
5. In this research, when the equal lateral load is subjected to the specimen under uniaxial tensile loading, the stress intensity factors in the case of $\beta = 0^o$ are not changed much, but the values of K_I / K_0 are increased, and those of K_{II} / K_0 become almost zero when $\beta = 15^o \sim 45^o$.
6. As the inclined angle of crack increases, under biaxial tensile loading, the values of K_I / K_0 become smaller, but there is little difference.

Acknowledgment

This research was supported by Yeungnam university research grants in 2007.

References

[1] T. H. H. Pian, P. Tong and C. H. Luk, Elastic Crack Analysis by a Finite Element Hybrid Method, *3rd Conf. Matrix Meth. Struct. Mech*, Wright-Patterson Air Force Base, Ohio (1971).

[2] K. K. Chandrashekhara and K. Jacob, Experimental Numerical Hybrid Technique for Stress Analysis of Orthotropic Composites, Edited by Hollister, *Applied Science Publication* (1977) 67-78.

[3] C. W. Smith, D. Post, G. Hiatt and G. Nicoletto, Displacement Measurements Around Cracks in Three dimensional Problems by a Hybrid Experimental Technique, *Exp. Mech*. 23 (1983) 15-20.

[4] D. C. Shin, J. S. Hawong, H. J. Lee, J. H. Nam and O. S. Kwon, Application of Transparent Photoelastic Experiment Hybrid Method to the Fracture Mechanics of Isotropic Material, *Trans. Korea Soc. Mech. Eng. (Series A)* 22 (1998) 834-842.

[5] D. C. Shin, J. S. Hawong, J. H. Nam, H. J. Lee and O. S. Kwon, Application of Transparent Photoelastic Experiment Hybrid Method to the Fracture Mechanics of Orthotropic Material, *Trans. Korea Soc. Mech. Eng. (Series A)* 22 (1998) 1036-1044.

[6] J. S. Hawong, D. C. Shin and H. J. Lee, Photoelastic Experimental Hybrid Method for Fracture Mechanics of Anisotropic Material, *Experimental Mechanics* 41 (2001) 92-99.

[7] R. Y. Kim and A. S. Crasto, Failure of Carbon Fiber-Reinforced Epoxy Composites under Combined Loading, *Proceedings of the Ninth International Conference on Composite Materials(ICCM IX)* V (1993) 15-22.

[8] S. R. Swanson and A. P. Christoforou, Response of Quasi-Isotropic Carbon/Epoxy Laminates to Biaxial Stress, *Journal of Composite Materials* 20 (1986) 457-471.

[9] S. R. Swanson, Biaxial Failure Criteria for Toughened Resin Carbon/Epoxy laminates, *Proceedings of the American Society for Composites 7th Technical Conference* (1992) 1075-1083.

[10] W. K. Lim, S. Y. Choi and B. V. Sankar, Biaxial Load Effects on Crack Extension in Anisotropic Solids, *Engineering Fracture Mechanics* 68 (2001) 403-416.

[11] A. Shimamoto, J. H. Nam, T. Shimomura and E. Umezaki, Determination of SIF in isotropic and anisotropic body by the Photoelastic and Caustics Methods under Various Load Ratios, *Key Engineering Materials* 183-187 (2000) 115-120.

[12] D. C. Shin, B. G. Nam, J. H. Nam, J. S. Hawong and K. Watanabe, A Study on the Cracked Specimen for Biaxial Tensile Loading Test, *Key Engineering Materials* 326-328 (2006) 1331-1334.

[13] N. I. Muskhelishvili, *Some Basic Problems of the Mathematical Theory of Elasticity* (1933), English translation, 4th Edition, P. Noordhoff Ltd., Groningen, Netherlands (1963).

[14] R. C. Sampson, A Stress-Optic Law for Photoelastic Analysis of Orthotropic Composites, *Exp. Mech*. 10 (1970) 210-215.

[15] J. H. Nam, A. Shimamoto and T. Shimomura, Development of Hydraulic Servo Dynamic Biaxial Loading Device, *Journal of the Japanese Society for Non-Destructive Inspection* 52 (2003) 349-354.

[16] J. F. Doyle, S. Kamle and J. Jakezaki, Error Analysis of Photoelasticity in Fracture Mechanics, *Exp. Mech*. 21 (1981) 429-435.

Dong-Chul Shin received the B.S., M.S. and Ph.D. degrees in Mechanical Engineering from Yeungnam University in 1995, 1997 and 2001, respectively. Dr. Shin studied at the University of Tokyo, Japan, for three years (from April, 2005 to January, 2008) as a Post-Doctoral fellow (supported by Korea Research Foundation (KRF) and Japan Society for the Promotion of Science (JSPS)).

Dr. Shin is currently a Research Professor at the School of Mechanical Engineering at Pusan National University, Korea. His research interests include the static and dynamic fracture mechanics, stress analysis, and fracture criteria of piezoelectric ceramics, etc.

Jai-Sug Hawong received a B.S. in Mechanical Engineering from Yeungnam University in 1974. Then he received his M.S. and Ph.D. degrees from Yeungnam University in Korea in 1976 and from Kanto Gakuin University in Japan in 1990, respectively. Prof. Hawong is currently a professor at the School of Mechanical Engineering at Yeungnam University, in Gyeongsan city, Korea. He is currently serving as vise-president of Korea Society Mechanical Engineering. His research interests are in the areas of static and dynamic fracture mechanics, stress analysis, experimental mechanics for stress analysis and composite material etc.